

## Improved projected Green's function approach to electron tunneling lifetime calculations in quantum wells

Hong-Shuai Tao,<sup>1</sup> Rundong Zhao,<sup>1</sup> Yanoar Pribadi Sarwono,<sup>1,2</sup> and Rui-Qin Zhang<sup>1,2,\*</sup>

<sup>1</sup>*Beijing Computational Science Research Center, Beijing 100193, China*

<sup>2</sup>*Department of Physics, City University of Hong Kong, Hong Kong SAR, China*

(Received 14 April 2017; revised manuscript received 10 October 2017; published 20 December 2017)

We demonstrate that the use of an optimal initial state of a wave function generated using Lanczos method allows the previously proposed projected Green's function approach to predict the tunneling lifetime of a particle crossing a double quantum well with a considerably improved accuracy. It is further revealed that the electron tunneling lifetime of such system depends linearly or quadratically on the barrier thickness or the well width. We also investigate the asymmetric double quantum well structure and find that the electron tunneling lifetime in it is strongly dependent on barrier thickness. Finally, we discuss the possible experimental designs to observe the above-mentioned tunneling features.

DOI: [10.1103/PhysRevB.96.235428](https://doi.org/10.1103/PhysRevB.96.235428)

Tunneling of carriers in semiconductor heterostructures has attracted enormous interest in both experimental and theoretical research, especially the tunneling current through the double-barrier potential of symmetric or asymmetric structures [1–4]. Numerous phenomena have been observed in such systems, such as the negative differential resistance, the current-voltage response, and the Josephson effect [5–7]. In recent decades, quantum well (QW) structure based devices have emerged and been widely used, i.e., QW-based optoelectronic devices, multiple QW semiconductor lasers, quantum structures for optical modulation, and quantum interference devices [8–12]. The accurate measurement of the tunneling times of electrons in double-well quantum systems has been a long-lasting significant issue, as the tunneling time is not only an important parameter in evaluating the performance of different electronic devices but also a fundamental physics problem that has been debated for more than 80 years [13,14]. The present paper does not discuss the controversy [15,16] of the definition of tunneling time, but aims at dealing with the commonly observable quantity: tunneling lifetime.

Experimentally, the electron tunneling lifetime in a QW system can be detected indirectly, such as by monitoring the decay of the electron localized between two barriers [17]; in theory, the tunneling lifetime of an electron's wave function can be calculated directly: many theoretical tools have been employed for such purpose, e.g., the argument principle method approach (APM) [18] and the transmission line analogy method [19], both of which try to find the roots of the wave function and can get the lifetime effectively in symmetric double-barrier systems and other simple cases. However, for the asymmetric cases and multibarrier cases, the roots will be much more complicated and even impossible to find out. On this aspect, the formerly proposed projected Green's function (PGF) method [20–23] is better, as it avoids solving the wave function directly and maps the system to a matrix to get eigenvalues and eigenvectors: it can evaluate the tunneling lifetime by directly treating the imaginary part of a

Green's function, regardless of the complexity of the system or structure.

In the PGF scheme, a tunneling particle is localized in a quantum well at the beginning and is supposed to tunnel through the barriers at  $t > 0$ . This is a dynamics process which calls for the solution of several complicated problems such as finding complex roots of nonlinear equations, treating the time-dependent Green's function, etc. In previous theoretical works, the APM method was used to treat this problem. It can extract all the complex solutions by using the argument principle method to solve the Schrödinger equation. However, when the barrier structure is extended from double-barrier to multibarrier cases, or when the symmetry of the structure is broken, the roots of the wave function will be much more difficult to find out, and in most cases it is impossible to deal with. In this paper, in combination with the Lanczos method [24], we investigate the projected Green's function method for realizing the optimal initial wave function [24]. Assuming a decay phase of the wave function which is affected by both electron tunneling effect and electron scattering effect from phonons or impurities, after applying Fourier transformation, we convert the original time-dependent Green's function into an energy-dependent Green's function. The tunneling lifetime can be obtained from the imaginary part of the Green's function in energy space. In the process of solving PGF, we exploit the Lanczos method (in building the eigenfunction) which makes the results much more precise.

Consider a one-dimensional double-barrier quantum well system with the length  $L$ , the barrier thickness  $B_1$  and  $B_2$ , and the well width  $W$ , as shown in Fig. 1. The standard Schrödinger equation of the electron in it can be written as

$$H\psi_i(x) = -\frac{\hbar^2}{2m}\frac{\partial^2}{\partial x^2}\psi_i(x) + V(x)\psi_i(x) = E_j\psi_i(x) \quad (1)$$

where  $m$  denotes the effective mass of the electron,  $\psi_i(x)$  is the eigenfunction with eigenvalue  $E_i$ , and  $V(x)$  is the potential that contains one well and two barriers. Equation (1) satisfies the boundary condition  $\psi_i(x=0) = \psi_i(x=L) = 0$ , where index  $i = 1, 2, \dots$  labels different eigenstates. We express the

\*Corresponding author: [aprqz@cityu.edu.hk](mailto:aprqz@cityu.edu.hk)

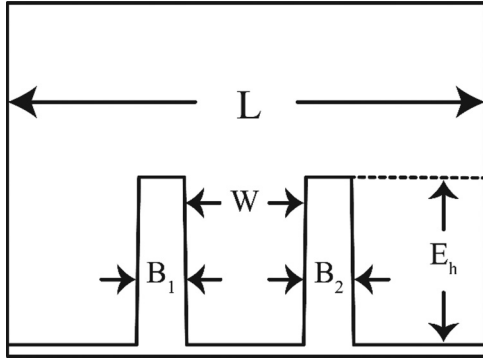


FIG. 1. The double-barrier QW structure: for the symmetric case,  $B_1 = B_2$ ; for the asymmetric case,  $B_1 \neq B_2$ .

originally localized wave function as

$$\phi(x,0) = \sum_i c_i \psi_i(x), \quad (2)$$

$$\sum_i c_i^* c_i \frac{1}{E + i\delta - E_i} = \langle \phi | G | \phi \rangle = \int_0^L \int_0^L \phi_i^*(x) G(x, x', E + i\delta) \phi_i(x') dx dx'. \quad (6)$$

Here  $\langle \phi | G | \phi \rangle$  is the so-called PGF, in which the Green's function  $G(x, x', E)$  is defined as

$$(E - \hat{H})G(x, x', E) = \delta(x - x'). \quad (7)$$

Substituting Eq. (7) into Eq. (6) results in

$$\langle \phi | G | \phi \rangle = \langle \phi | \frac{1}{E + i\delta - \hat{H}} | \phi \rangle. \quad (8)$$

To deal with Eq. (8) we adopt a recursion method combined with the Lanczos method to translate the Hamiltonian  $\hat{H}$  to a matrix form [21,24,25], and the PGF can be written as

$$\langle \phi | G | \phi \rangle = G_0(E + i\delta) = \begin{pmatrix} E + i\delta - a_0 & -b_1 & 0 & \cdots \\ -b_1 & E + i\delta - a_1 & -b_2 & \cdots \\ 0 & -b_2 & E + i\delta - a_2 & \cdots \\ \vdots & \vdots & \vdots & \ddots \end{pmatrix}_{00}^{-1} \quad (9)$$

with  $a_i, b_i, i = 0, 1, 2, \dots, N-1$  being the recursion coefficients defined as follows:

$$\begin{aligned} \hat{H}\phi &= a_0\phi + b_1\phi_1, \\ \hat{H}\phi_i &= b_i\phi_{i-1} + a_i\phi_i + b_{i+1}\phi_{i+1}, \\ &\dots \end{aligned} \quad (10)$$

Here  $\phi, \phi_1, \dots, \phi_{N-1}$  is a set of wave functions that are localized in the system, and  $a_i$  and  $b_i$  describe the coupling of each environment to itself and its neighbors [21,25]. We denote the determinant of the matrix  $\langle \phi | G | \phi \rangle$  with the first  $i$  rows and columns as  $D_i(E + i\delta)$ . Then, Eq. (9) is simplified as

$$\langle \phi | G | \phi \rangle = G_0(E + i\delta) = \frac{D_1(E + i\delta)}{D_0(E + i\delta)}. \quad (11)$$

By expanding the determinants  $D_0(E + i\delta)$  in the denominator, we easily get

$$G_0(E + i\delta) = \frac{D_1(E + i\delta)}{(E + i\delta - a_0)D_1(E + i\delta) - b_1^2 D_2(E + i\delta)} = \frac{1}{E + i\delta - a_0 - b_1^2 \frac{D_2(E + i\delta)}{D_1(E + i\delta)}}. \quad (12)$$

Here we define  $D_2(E + i\delta)/D_1(E + i\delta)$  as  $G_1(E + i\delta)$ .

and the time-dependent wave function  $\phi(x, t)$  as

$$\phi(x, t) = \sum_i c_i \psi_i(x) \exp(-iE_i t/\hbar), \quad (3)$$

where  $t \geq 0$  for physical reasons. In the tunneling escape process, as the wave function  $\phi(x, t)$  changes, the time-dependent wave amplitude of the original wave function  $\phi(x, 0)$  contained in  $\phi(x, t)$  can be defined as

$$\langle \phi(x, 0) | \phi(x, t) \rangle = \int_0^L \phi^*(x, 0) \phi(x, t) dx = \sum_i c_i^* c_i e^{-iE_i t/\hbar}. \quad (4)$$

After performing a Fourier transform, we get

$$\int_{-\infty}^{\infty} \langle \phi(x, 0) | \phi(x, t) \rangle e^{iEt/\hbar} dt = i\hbar \sum_i c_i^* c_i \frac{1}{E - E_i + i\delta} \quad (5)$$

where  $\delta$  is a small number added to ensure the convergence. In order to relate Eq. (5) to the Green's function  $G(x, x', E + i\delta)$  [20], we derive the following formula:

For the system we are concerned with, it is rather complicated to get  $\varphi_i$  directly. Thus, we approximate the Hamiltonian by dividing the wave function  $\varphi_i$  into  $M$  pieces. Therefore  $\varphi_i$  can be written as  $\varphi_i(x_k)$  and here  $x_k (k = 1, 2, 3, \dots, M)$  denotes the discrete position values of the system, with the length of each piece  $\Delta = L/(M - 1)$ . Under this approximation,  $a_i$ ,  $b_i$ , and the wave function  $\varphi_i$  in Eq. (9) are described as follows:

$$W_i(x_k) = -\frac{\hbar^2}{2m\Delta^2}[\varphi_i(x_{k+1}) - 2\varphi_i(x_k) + \varphi_i(x_{k-1})] + V(x_k)\varphi_i(x_k), \quad a_i = \sum_k \varphi_i(x_k)W_i(x_k)\Delta, \quad (13)$$

$$b_{i+1}^2 = \sum_k |W_i(x_k) - a_i\varphi_i(x_k) - b_i\varphi_{i-1}(x_k)|^2\Delta, \quad \varphi_{i+1}(x_k) = \frac{1}{b_{i+1}}[W_i(x_k) - a_i\varphi_i(x_k) - b_i\varphi_{i-1}(x_k)].$$

Now, all the coefficients of PGF have been calculated. However, the eigenvector  $\phi$ , which depends on the order of the  $H$  matrix we selected, may be imprecise, because in the PGF we only choose the fixed value of  $M$  and get the eigenvalue and eigenvector from only one diagonalization. To reach a higher accuracy, we adopt the Lanczos method to make the eigenvector  $\phi$  much more precise [24], the procedure of which is given as follows.

(1) Choose a set of random numbers as the wave vector (also, the order of the vector is chosen as  $M$ ), and construct the  $H$  matrix, following the Lanczos technique.

(2) Diagonalize of the matrix and obtain the eigenvalues and the eigenvector.

(3) Use the new eigenvector to rebuild the  $H$  matrix and again get another group of eigenvalues and eigenvector.

(4) Repeat steps 2 and 3 iteratively and compare these two groups of values (obtained from steps 2 and 3, respectively) at each iteration: if the eigenvalue converges, stop the iteration and set the eigenvector as  $\phi$ , which will be used in the PGF.

Then we get the coefficients  $a_i$ ,  $b_i$  using Eq. (13) as well as the precise wave vector  $\phi$  using Lanczos analysis. Equation (12) can be rewritten as

$$G_0(E + i\delta) = \frac{1}{E + i\delta - a_0 - b_1^2 G_1(E + i\delta)} = \frac{1}{E - a_0 - b_1^2 \text{Re}[G_2(E + i\delta)] + i\delta - ib_1^2 \text{Im}[G_1(E + i\delta)]}. \quad (14)$$

In the denominator of Eq. (14),  $\delta$  is a very small but finite positive value that has several interpretations. Mathematically speaking, it ensures the convergence of the Fourier transform of the Green's function, but physically this  $\delta$  can reduce the decay lifetime of the localized wave function which represents the effect of inelastic scattering, as illustrated in the literature: for the quantum well structure, the electron will be scattered by impurities or phonons, and the changes from its initial state into another state are characterized by the parameters of  $\delta$  or  $\tau_b$  (see later in the text) [18,26]. We assume  $i\delta$  to be a phase factor that is added to the time-dependent Green's function in the form of  $\langle \phi | G | \phi \rangle \sim \exp(-iE_r t/\hbar - t/2\tau)$ , where  $E_r$  is the energy of the resonant level. The total lifetime  $\tau_t$  is multiplied by a factor of 2 due to the accumulated time shift when the wave packet is moving toward the potential barrier and when it is moving away from the barrier [13,27]. Through this approximation, the PGF will have a Lorentzian peak as follows:

$$\langle \phi | G | \phi \rangle = \frac{1}{E - E_i + i\frac{\hbar}{2\tau_t}}. \quad (15)$$

Comparing this equation with Eq. (14), we directly get the expression of  $\tau_t$ :

$$\frac{1}{\tau_t} = \frac{2\{\delta - b_1^2 \text{Im}[G_1(E_i + i\delta)]\}}{\hbar} = \frac{1}{\tau_b} + \frac{1}{\tau}, \quad (16)$$

where  $\tau_t$  denotes the total lifetime of the electron in the system. It contains two parts: the tunneling lifetime through the barriers and the decay time  $\tau_b$  due to the imaginary part  $i\delta$ . Their expressions are given by

$$\tau_b = \frac{\hbar}{2\delta}, \quad \tau = \frac{\hbar}{-2b_1^2 \text{Im}[G_1(E_i + i\delta)]}. \quad (17)$$

The lifetime  $\tau$  in Eq. (17) depends on the value of  $G_1(E_i + i\delta)$  which is a matrix consisting of coefficients  $a_i$  and  $b_i$ . It is valid and well defined only when  $G_1$  is a function that is independent of energy  $E$ . To satisfy this condition,  $\delta$  should be larger than the energy-level spacing of the heterostructure to make sure that  $G_1$  will not change much when we vary the value of energy  $E$ . For systems considered here,  $\delta$  is chosen to be 2 meV to satisfy the convergence in the Fourier transform and to obey the rules of longitudinal optical phonons and carrier-carrier Coulomb interaction in the experiment [22,28]. The variance of the imaginary part of the PGF and  $G_1$  according to the changes of  $E$  is plotted in Fig. 2, indicating a valid value of  $\delta$ .

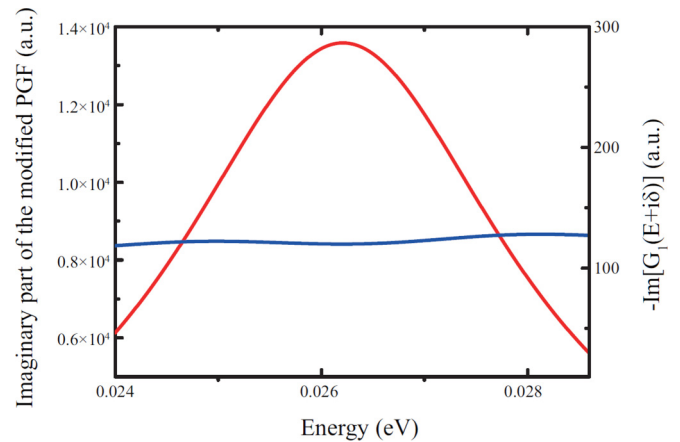


FIG. 2. Imaginary part of the modified PGF (red line) and  $-\text{Im}[G_1(E+i\delta)]$  (blue line) as a function of energy in the double-barrier system shown in Fig. 1.

TABLE I. Tunneling lifetime of a double-barrier case obtained with PGF only, with PGF combined with Lanczos method, and with APM [18].

$W_1$ (Å)	$B_1 = B_2$ (Å)	$\tau$ PGF only (ps)	$\tau$ PGF + Lanczos (ps)	APM (ps)
100	20	2.500	2.155	2.1
100	40	131.2	114.1	111.48
50	20	0.273	0.234	0.226
50	40	10.70	9.423	8.935

The performance of the combination of PGF and Lanczos method in the symmetric double-barrier QWs is checked by comparing the calculated electron tunneling lifetime with the result of the APM method, which is shown in Table I and Fig. 3. Using the barrier structure shown in Fig. 1 with the barrier height  $E_h = 0.4$  eV and the electron mass  $0.1m_e$ , we explored several typical cases: the well width  $W = 100$  or  $50$  Å and the barrier thickness  $B_1 = B_2 = 20$  or  $40$  Å, as listed in Table I. Apparently, the barrier thickness significantly affects the tunneling lifetime: as it increases, the tunneling lifetime should be longer, as expected from intuition. The tunneling lifetime also increases as the well width enlarges, according to Fig. 3, which is obtained using the fixed barrier width. Compared with the results of APM, the PGF approach gives a reliable tunneling lifetime with acceptable slight difference. The Lanczos method for generating the eigenvector  $\phi$  leads to more exact results, cutting the percentage of difference from 20 to less than 5%.

Figure 4 shows the tunneling lifetime  $\tau$  as a function of the well width at different values of the fixed barrier thickness  $B$  (for symmetric case  $B = B_1 = B_2$ ). It is found that  $\tau$  will increase continuously as we increase  $W$ , meaning that the electron spends more time dwelling between the two barriers. This can be interpreted from the viewpoint of the distribution probability of the electron: a larger  $W$  provides a more spacious region for the electron wave function to diffuse, leading to a more even distribution of the electron, and thus diminishes the

probability of tunneling out (the proportion of the probability for an electron to be distributed near to the barrier is lower). Comparison between these four different values of  $B$  shows that larger thickness values cause  $\tau$  to grow much faster than it does with small thickness values. With a small value of  $B = 35$  Å, the increase seems linear, while a larger value of  $B = 50$  Å shows an exponential increase. The barrier thickness affects  $\tau$  strongly in the symmetric system as seen from Fig. 5. Figure 5(a) shows  $\tau$  as a function of  $B$  with different values of fixed  $W$ . Furthermore, we plot the result of the tunneling lifetime as a function of the well width while the barrier thickness is kept at the value of  $B = 50$  Å in Fig. 5(a) (the purple dashed line). Comparison among the four curves shows that the barrier thickness impacts the lifetime more strongly than the well width. Then we choose a special case of the fixed well width  $W = 50$  Å [shown in Fig. 5(b)] for detailed exploration. At  $B < 45$  Å, the tunneling lifetime increases almost linearly, because the very thin barriers fit the conditions of Tsuchiya *et al.*'s work [17], in which the tunneling lifetime can be indicated by the photoluminescence (PL) decay time, and the increasing rate displays a similar trend to a classic Newtonian velocity which is a function of time and length. We call this region the “linear region” or the “classical region.” On the other hand, the increasing rate suddenly becomes very large at  $B > 45$  Å, and the curve behaves like an exponential function. We call this part “the exponential region,” in which the tunneling lifetime is very

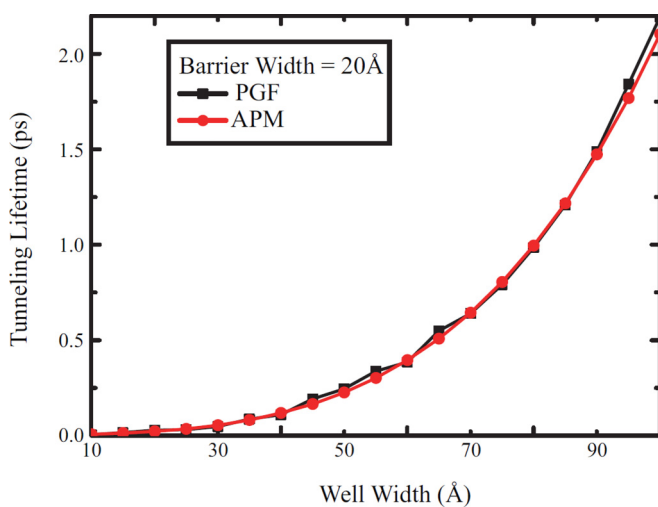


FIG. 3. A comparison of the tunneling lifetime as a function of the well width obtained with the PGF and APM method. The value of the barrier thickness is kept at  $B = 20$  Å.

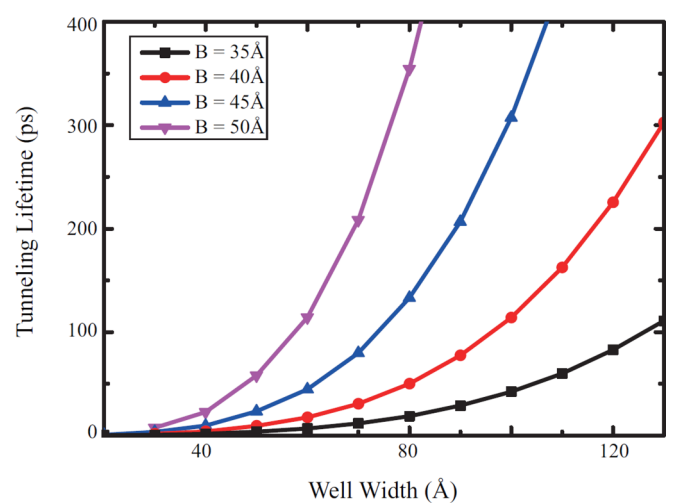


FIG. 4. Tunneling lifetime  $\tau$  as a function of the well width  $W$  with a fixed barrier thickness  $B$ . Different colors indicate the different barrier thicknesses in the symmetric double-barrier system.

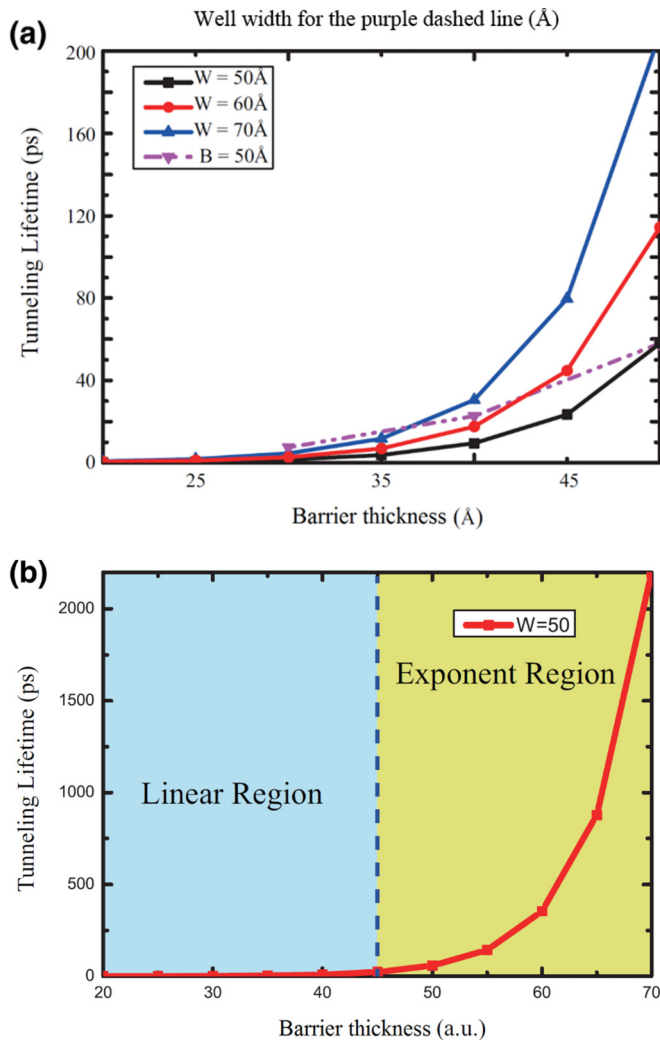


FIG. 5. (a) Tunneling lifetime  $\tau$  as a function of the barrier thickness  $B$  with a fixed well width  $W$  shown with the solid lines of different colors. The purple dashed line shows  $\tau$  as a function of the well width  $W$  with the barrier thickness  $B = 50 \text{ \AA}$ . (b) Tunneling lifetime as a function of the barrier thickness  $B$  when  $W = 50 \text{ \AA}$ . The two colors show two types of increase.

sensitive to the barrier thickness. The amplitude of the wave function will decrease exponentially as we increase the value of the thickness, which causes the curve to behave as shown in Fig. 5(b).

Asymmetric QWs are structures that other theoretical methods are incapable of but that are within the capability of PGF. We then consider an asymmetric double-barrier case ( $B_1 \neq B_2$ ), to study how the tunneling lifetime is affected by the breakdown of symmetry. Figure 6 demonstrates the results of the electron tunneling lifetime as a function of barrier thickness  $B_2$  with fixed  $B_1$  and fixed well width  $W$ . As  $B_2$  is enlarged, the tunneling lifetime increases, and the steepest slope with the largest increasing rate occurs at  $B_2 = 40 \text{ \AA}$  (indicated by the black dashed line, which divides Fig. 6 into two parts: zone I and zone II). After that, the increasing slows down, and tends to a constant at  $B_2 > 80 \text{ \AA}$ . It is rational that the right barrier is very thin in the region of zone I, thus the electron will traverse it much more easily, viz., the probability

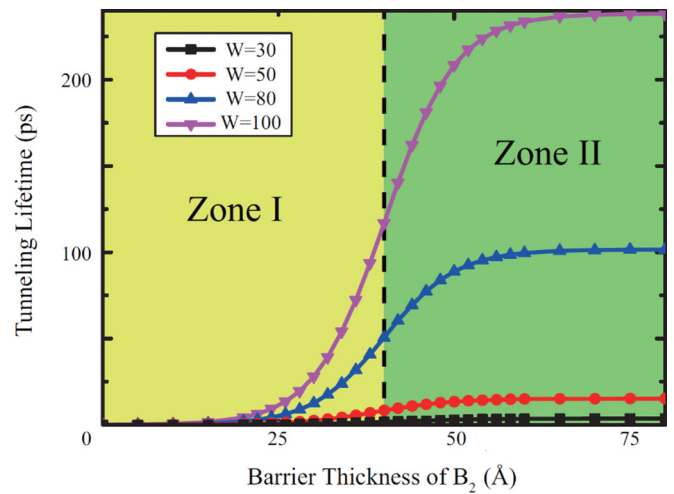


FIG. 6. The tunneling lifetime as a function of the right barrier thickness  $B_2$ , with the fixed left barrier thickness  $B_1$  and the fixed well width  $W$ . The black dashed line in the middle represents the symmetric case  $B_1 = B_2 = 40 \text{ \AA}$ . Zone I denotes the region  $B_2 < 40 \text{ \AA}$  and zone II denotes the region  $B_2 > 40 \text{ \AA}$ .

for an electron to tunnel in this direction is very high. So, the tunneling lifetime increases quickly as we keep enlarging the thickness value of  $B_2$ . For the case of the thickness value  $B_2$  larger than  $40 \text{ \AA}$ , the tunneling time keeps on increasing but not that quickly, because the tunneling electron will meet a growing resistance on the right side; thus it has an appreciable probability to choose the left barrier to escape. At  $B_2 > 80 \text{ \AA}$ , the tunnel on the right is nearly prohibited and the electron wave has a significant large probability to tunnel out from left. Increasing  $B_2$  then will not affect the tunneling lifetime considerably. Therefore, we see a horizontal line beyond  $B_2 = 80 \text{ \AA}$ .

Molecular-beam epitaxy, which is a convenient method for controlling the barrier thickness and well width, is suggested for the experimental implementation of the double-barrier AlAs-GaAs-AlAs heterostructures. The double-barrier structure can be grown on a semi-insulating GaAs substrate: the GaAs quantum well with the well width  $W$  is located in the middle of two  $\text{Al}_x\text{Ga}_{1-x}\text{As}$  barriers with the respective barrier thickness  $B_1$  and  $B_2$ ; the whole double-barrier system is bounded by a GaAs cap layer and a GaAs buffer layer, which have sufficient thickness. This system allows us to measure the escape time of an electron in the well by time-resolved PL. We are able to modify the GaAs layers to control the well width  $W$  and to vary the  $\text{Al}_x\text{Ga}_{1-x}\text{As}$  layers so as to adjust the barrier thickness  $B_1$  and  $B_2$ . We suggest choosing very thin barriers ( $B < 80 \text{ \AA}$ ) to fit the conditions of this experiment [17].

In conclusion, we investigated the tunneling lifetime in several typical double-barrier structures of semiconductor heterostructures, using the PGF method combined with the Lanczos technique. The relationship between the tunneling lifetime and well, barrier width, and thickness is explored, showing that not only the barrier thickness but also the well width has a strong influence on the system. The symmetric double-barrier case is further considered, showing an S-shape curve of the tunneling lifetime as a function of the one-side barrier thickness, indicating a good agreement with the PL

decay time in experiments when the barrier is very thin. Finally, we propose an experimental protocol of the symmetric or asymmetric double-barrier structures to observe these phenomena in future research.

### ACKNOWLEDGMENTS

This work was supported by the NSAF U1530401. We also acknowledge the computing resource of the Tianhe2-JK cluster at the Beijing Computational Science Research Center.

- 
- [1] T. B. Norris, X. J. Song, W. J. Schaff, L. F. Eastman, G. Wicks, and G. A. Mourou, *Appl. Phys. Lett.* **54**, 60 (1989).
  - [2] M. G. W. Alexander, M. Nido, W. W. Rühle, and K. Köhler, *Phys. Rev. B* **41**, 12295(R) (1990).
  - [3] E. N. Glytsis, T. K. Gaylord, and K. F. Brennan, *J. Appl. Phys.* **70**, 3920 (1991).
  - [4] J. Hwang and J. D. Phillips, *Phys. Rev. B* **83**, 195327 (2011).
  - [5] L. L. Chang, L. Esaki, and R. Tsu, *Appl. Phys. Lett.* **24**, 593 (1974).
  - [6] V. J. Goldman, D. C. Tsui, and J. E. Cunningham, *Phys. Rev. Lett.* **58**, 1256 (1987).
  - [7] B. D. Josephson, *Phys. Lett.* **1**, 251 (1962).
  - [8] D. A. B. Miller, D. S. Chemla, T. C. Damen, A. C. Gossard, W. Wiegmann, T. H. Wood, and C. A. Burrus, *Phys. Rev. B* **32**, 1043 (1985).
  - [9] C. Weisbuch and B. Vinter, *Quantum Semiconductor Structures: Fundamentals and Applications* (Academic Press, London, 1991).
  - [10] D. A. G. Deacon, L. R. Elias, J. M. J. Madey, G. J. Ramian, H. A. Schwettman, and T. I. Smith, *Phys. Rev. Lett.* **38**, 892 (1977).
  - [11] T. Sollner, W. Goodhue, P. Tannenwald, C. Parker, and D. Peck, *Appl. Phys. Lett.* **43**, 588 (1983).
  - [12] F. Capasso, K. Mohammed, and A. Y. Cho, in *Electronic Structure of Semiconductor Heterojunctions* (Springer, New York, 1988), pp. 99–115.
  - [13] A. S. Landsman and U. Keller, *Phys. Rep.* **547**, 1 (2015).
  - [14] J. G. Muga, R. Sala Mayato, and I. L. Egusquiza, *Time in Quantum Mechanics* (Springer-Verlag, Berlin, Heidelberg, 2008).
  - [15] R. Landauer, *Rev. Mod. Phys.* **66**, 217 (1994).
  - [16] G. Orlando, C. R. McDonald, N. H. Protik, G. Vampa, and T. Brabec, *J. Phys. B* **47**, 204002 (2014).
  - [17] M. Tsuchiya, T. Matsusue, and H. Sakaki, *Phys. Rev. Lett.* **59**, 2356 (1987).
  - [18] E. Anemogiannis, E. N. Glytsis, and T. K. Gaylord, *IEEE J. Quantum Electron.* **29**, 2731 (1993).
  - [19] A. Anwar, A. Khondker, and M. R. Khan, *J. Appl. Phys.* **65**, 2761 (1989).
  - [20] G. Barton, *Elements of Green's Functions and Propagation: Potentials, Diffusion, and Waves* (Oxford University Press, Oxford, 1989).
  - [21] R. Haydock, *Comput. Phys. Commun.* **20**, 11 (1980).
  - [22] K. S. Chan and R. Q. Zhang, *IEEE J. Quantum Electron.* **34**, 2179 (1998).
  - [23] R. Zhao, Y. P. Sarwono, and R.-Q. Zhang, *J. Chem. Phys.* **147**, 064109 (2017).
  - [24] E. Dagotto, *Rev. Mod. Phys.* **66**, 763 (1994).
  - [25] R. Haydock, V. Heine, and M. Kelly, *J. Phys. C* **8**, 2591 (1975).
  - [26] A. Douglas Stone and P. A. Lee, *Phys. Rev. Lett.* **54**, 1196 (1985).
  - [27] T. B. Bahder, C. A. Morrison, and J. D. Bruno, *Appl. Phys. Lett.* **51**, 1089 (1987).
  - [28] M. Asada, *IEEE J. Quantum Electron.* **25**, 2019 (1989).